


Article

Terminal Impact Angle Control Guidance Law Considering Target Observability

Bin Li ¹ , Pan Tang ², Haotian Xu ¹ and Duo Zheng ^{3,*}

¹ Department of Automation, Tsinghua University, Beijing 100084, China; binli626@mail.tsinghua.edu.cn (B.L.); xuht21@mails.tsinghua.edu.cn (H.X.)

² Beijing Institute of Aerospace Systems Engineering, Beijing 100076, China; pingyuantangpan@163.com

³ School of Aerospace Engineering, Beijing Institute of Technology, Beijing 100081, China

* Correspondence: zhengduohello@126.com

Abstract: The problem of the terminal impact angle control guidance law, considering the target observability for passive guidance with bearing-only measurement, is investigated in this paper. Modified line-of-sight (LOS) angle error dynamics and their closed-loop analytical solution are developed to enhance the target observability, and then their characteristics are studied, which makes the LOS angular rate oscillate in the early stage. The terminal impact angle control guidance law with the global sliding mode is designed to eliminate the approaching stage of sliding mode control, which makes the system robust throughout the entire process of control. Finally, numerical simulations are presented to demonstrate the performance of the proposed guidance law under various conditions, which achieves the desired results.

Keywords: terminal impact angle control; target observability; line-of-sight angle error dynamics; global sliding mode



Citation: Li, B.; Tang, P.; Xu, H.; Zheng, D. Terminal Impact Angle Control Guidance Law Considering Target Observability. *Aerospace* **2022**, *9*, 193. <https://doi.org/10.3390/aerospace9040193>

Academic Editor: Gokhan Inalhan

Received: 3 March 2022

Accepted: 1 April 2022

Published: 3 April 2022

Publisher's Note: MDPI stays neutral with regard to jurisdictional claims in published maps and institutional affiliations.



Copyright: © 2022 by the authors. Licensee MDPI, Basel, Switzerland. This article is an open access article distributed under the terms and conditions of the Creative Commons Attribution (CC BY) license (<https://creativecommons.org/licenses/by/4.0/>).

1. Introduction

Without the consideration of target maneuvers and the time delay between guidance and control systems, the well-known proportional navigation guidance (PNG) law, which can be regarded as an optimal guidance law when the navigation ratio is set as 3, has been used in various engineering practices successfully [1]. In some applications, in addition to hitting the target, it may also be desirable to shape the missile trajectory near impact. For example, it is expected to hit the weak part of the target to enhance the missile's attack effect, such as the anti-tank missile attacking the target with a large terminal impact angle to complete the high-efficiency damage [2,3]. Reference [4] introduced the Cauchy–Schwarz inequality to analyze the guidance problem and proposed an impact angle constrained optimal guidance law called the trajectory shaping guidance (TSG) law to achieve a better performance. Reference [5] proposed a new homing guidance law that can attack the target with a desired impact angle. Essentially, it is a variation of the PNG law, which includes a supplementary time-varying bias. Reference [6] studied the bias guidance law without the remaining flight time and added an angle constraint bias term based on the PNG law to control the terminal impact angle by changing the guidance command. Reference [7] proposed an optimal-control-based guidance law considering the field-of-view constraint for the practical implementation of impact angle control guidance. Reference [8] designed an optimal guidance law with a constraint on the impact angle and acceleration limit.

Owing to the time-varying aerodynamical coefficients, target maneuvers and external disturbances, the dynamical characteristics of missile guidance and control system are full of nonlinearities and uncertainties. To handle this problem, in the literature [9–12], many works design nonlinear guidance laws based on nonlinear control theories that hold the properties of a high precision, disturbance resistance and strong robustness. Among nonlinear control theories, the sliding mode control (SMC) theory has been widely used

in guidance law design works. Reference [13] used the adaptive sliding mode method to design the guidance law, and the convergence speed of the sliding surface increases with the decrease in the relative distance between the missile and target. Reference [14] proposed a linear sliding mode guidance law that satisfied the stationary target and met the terminal impact angle constraint. Reference [15] designed the guidance law by the SMC method, which satisfied the terminal impact angle constraint and could improve the observability of a stationary or slow moving target. Although the above guidance laws can achieve an accurate interception, the target observability, one of the important factors for the passive seeker that can only measure the relative bearing or line-of-sight (LOS) angle, is not considered and discussed.

The target observability first proposed by Lingren and Gong [16] is determined by the relative target-missile geometry and motion relationships [17–19]. Specifically, for a passive bearing-only missile, the missile could maneuver under the guidance command to prevent the system state from being unobservable. It is known that the guidance law design, enhancing the target observability, can yield significant benefits for interceptors equipped with passive seekers [20]. A weaving guidance law was proposed in [21] for target observability improvement by introducing new virtual system states to be controlled. According to the principle of observability, because of its guidance principle, the target observability gradually decreases for passive seekers as the target approaches. Reference [22] proposed a biased PNG law to enhance the target observability for passive homing missile systems against a nonmaneuvering target. The target observability of the biased PNG law is related to the selection of the bias term. In order to adapt to the ballistic trajectory in order to control the terminal impact angle under the bias term, the biased PNG law has a certain target observability. However, the biased PNG law will become the PNG law when the LOS angular rate of the missile gradually converges to zero, and it will gradually decrease the target observability. Reference [23] developed a new optimal guidance law by maximizing the observability metric while minimizing the terminal miss distance, as well as the energy consumption. By intentionally utilizing the low damping ratio during the initial flight period, target observability improvement guidance for impact angle control can be found in [24]. Reference [25] suggested a linear quadratic guidance law that provides an oscillating trajectory to enhance the target observability, but it is formulated in a complicated guidance command and, thus, it is difficult to analyze its physical properties theoretically. Reference [26] proposed a new optimal guidance law for the passive guidance problem based on the relative bearing or LOS angle by the passive seeker, which considered the terminal miss distance, control energy and target observability, and took the integral of the LOS angular rate as the observability index of the target.

Considering the target observability, this paper proposes a new type of terminal impact angle control guidance law for the passive guidance problem. First, the observability criterion of the stationary target is given. Modified LOS angle error dynamics and their closed-loop analytical solution are studied to make the LOS oscillate to enhance the target observability. Next, the terminal impact angle control guidance law with the global sliding mode, considering the target observability, is designed. When the design parameter $k_2 > 2$ is obtained by analyzing the closed-loop analytical solution of the LOS angle error dynamics, the acceleration command of the guidance law can converge to zero at the guidance terminal.

The rest of this paper is organized as follows. First, missile–target relative kinematics are given in Section 2. Section 3 interprets the target observability and error dynamics, and the new type of guidance law for observability improvement is designed in Section 4. Then, some numerical simulation results are illustrated in Section 5. Finally, the conclusions of the whole paper are offered in Section 6.

2. Missile–Target Relative Kinematics

This paper considers a two-dimensional planar homing engagement geometry that is shown in Figure 1. As presented in the geometry, the inertial reference frame is denoted

as (X, Y) . Variables with subscripts of M and T denote those of the missile and target, respectively. λ and r represent the LOS angle and the missile–target relative range, respectively. θ represents the flight path angle of the missile defined in the inertial reference frame. The velocity and lateral acceleration of the missile are represented by V and a , respectively. Defining the target angle of view is the angle between the longitudinal axis of the missile and the line of sight of the missile. When the angle of attack is negligible, it can be expressed by the error angle σ of the velocity direction of the missile. θ_f represents the angle between the x-axis and the velocity direction of the missile when the missile hits the target. For simplicity, assume that the missile is flying with a constant velocity and that the target is fixed.

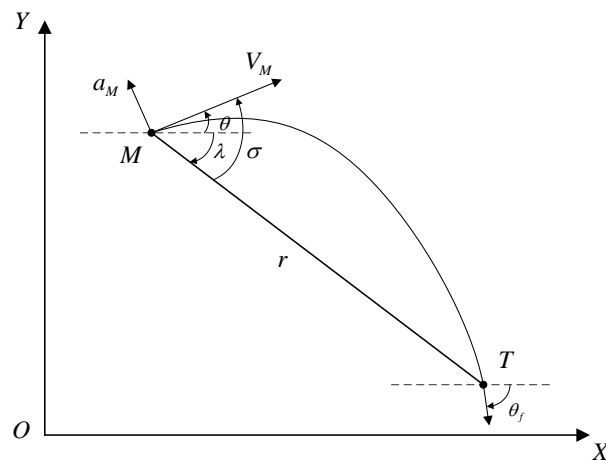


Figure 1. Planar engagement geometry.

The relative kinematics of the missile to target can be formulated as

$$\dot{r} = -V_M \cos \sigma \tag{1}$$

$$r\dot{\lambda} = -V_M \sin \sigma \tag{2}$$

$$\sigma = \theta - \lambda \tag{3}$$

The complementary equation defining the relationship between the flight path angle and normal acceleration is

$$\dot{\theta} = \frac{a_M}{V_M} \tag{4}$$

For a stationary target, $\theta_f = \lambda_f$. Therefore, the control of the terminal impact angle can be equivalently converted into the control of the terminal LOS angle. The control goal of the terminal impact angle constraint guidance law is to achieve $\dot{\lambda} \rightarrow 0, \lambda \rightarrow \lambda_d$ in a finite time, where λ_d is the terminal LOS angle.

Then, differentiating Equation (2) with respect to time yields

$$r\ddot{\lambda} = -2\dot{r}\dot{\lambda} - a_M \cos \sigma \tag{5}$$

Defining $e = \lambda - \lambda_d$ as the LOS angle error, we obtain

$$\dot{e} = \dot{\lambda} \tag{6}$$

denoting the uncertainty of the guidance system, variable x_1 and variable x_2 as d, e and \dot{e} , respectively. Among them, the uncertainty of the guidance system includes the model's model uncertainty and external disturbances. The LOS error dynamics equation, considering the uncertainty of the guidance system, can be expressed as

$$\dot{x}_1 = x_2 \quad (7)$$

$$\dot{x}_2 = \frac{-2r\dot{\lambda} - a_M \cos \sigma + d}{r} \quad (8)$$

Lemma 1. Suppose that, in the region $U \subset \mathbb{R}^n$, given a positive definite continuous function $V(x)$, if there are real numbers satisfying $a > 0$ and $b \in (0, 1)$ such that $\dot{V}(x) + aV^b(x) \leq 0$, then there exists a certain region $U_0 \subset \mathbb{R}^n$ such that $V(x)$ converges to the origin in a finite time, and the finite convergence time is

$$t_r \leq \frac{V^{1-b}(x_0)}{a(1-b)} \quad (9)$$

where $V(x_0)$ is the initial value of $V(x)$.

Lemma 2. Suppose $V(x)$ is a positive definite continuous function on $U \subset \mathbb{R}^n$. If there are real numbers satisfying $a > 0$, $b \in (0, 1)$ and $c > 0$ such that $\dot{V}(x) + cV(x) + aV^b(x) \leq 0$, then there exists a certain region $U_0 \subset \mathbb{R}^n$ such that $V(x)$ converges to the origin in a finite time, and the finite convergence time is

$$t_r \leq \frac{1}{c(1-b)} \ln \frac{cV^{1-b}(x_0) + a}{a} \quad (10)$$

where $V(x_0)$ is the initial value of $V(x)$.

3. Target Observability and Error Dynamics

The observability of the fixed target can be determined by the Gammian matrix [27]. When $t > t_0$, the Gammian matrix is represented as

$$D(t) = \int_{t_0}^t M^T(\tau)M(\tau)d\tau \quad (11)$$

where $M(t) = [-\sin \lambda(t) \quad \cos \lambda(t)]$. The target is observable when the matrix $D(t)$ is positive. In order to judge the observability of the target more easily and intuitively, the matrix $A(t)$ is defined as follows:

$$A(t) = \begin{bmatrix} M(t) \\ \dot{M}(t) \end{bmatrix} = \begin{bmatrix} -\sin \lambda(t) & \cos \lambda(t) \\ -\dot{\lambda}(t) \cos \lambda(t) & -\dot{\lambda}(t) \sin \lambda(t) \end{bmatrix} \quad (12)$$

When the matrix $A(t)$ is not full rank, the target is unobservable. To determine whether the matrix $A(t)$ is full rank, its determinant is

$$\det(A(t)) = \dot{\lambda}(t) \quad (13)$$

Therefore, the condition where the fixed target is observable is that the LOS angle rate is not zero. However, from the viewpoint of reducing the amount of the terminal miss distance, it is desirable for the terminal $\dot{\lambda}(t) = 0$. In order to satisfy both requirements at the same time, the LOS angle is oscillated near the desired terminal impact angle in the initial stage of guidance to ensure the observability of the target, and then the LOS angle rate is gradually converged to zero as the distance of the projectile decreases. Therefore, maximizing the value of $\int |\dot{\lambda}|$ is a practical way to increase the target observability. To realize this objective, this paper proposes the error dynamics equation by introducing a linear error term as

$$\ddot{e} + \frac{k_1 + k_2}{t_{go}} \dot{e} + \left(\frac{(k_1 + k_2)k_2}{t_{go}^2} + k_3 \right) e = 0 \quad (14)$$

where t_{go} is the time to go until the intercept and k_1, k_2 and k_3 are design parameters.

To interpret the physical meaning of the introduced error term, we rewrite (14) as an instantaneous linear time-invariant system:

$$\ddot{e} + 2\zeta\omega\dot{e} + \omega^2e = 0 \tag{15}$$

where

$$\zeta = \frac{k_1 + k_2}{2\sqrt{(k_1 + 1)k_2 + k_3t_{go}^2}}, \omega = \sqrt{\frac{(k_1 + 1)k_2}{t_{go}^2} + k_3} \tag{16}$$

The boundaries of ζ and ω are obtained from (16) as

$$\frac{k_1 + k_2}{2\sqrt{(k_1 + 1)k_2 + k_3t_f^2}} \leq \zeta \leq \frac{k_1 + k_2}{2\sqrt{(k_1 + 1)k_2}} \tag{17}$$

$$\sqrt{\frac{(k_1 + 1)k_2}{t_f^2} + k_3} \leq \omega \leq \infty$$

where t_f is the total flight time.

Analogous to the mass-spring-damper system, it follows from (16) that the initial natural oscillatory frequency ω increases and the initial damping ratio ζ decreases with the increase in k_3 . During the initial flight period, the large t_{go} enforces the term $k_3t_{go}^2$ to play a dominant role that affects the value of the damping ratio. During the entire homing engagement, t_{go} gradually converges to zero and, consequently, the term $(k_1 + 1)k_2$ will dominate over $k_3t_{go}^2$, which means that the modified error dynamics gradually converges to the original dynamics. Therefore, the damping ratio gradually increases from a small value to a large one as the interceptor approaches the target to generate the oscillatory LOS motion by choosing the parameter k_3 properly.

To provide better insights of the introduced biased term and analyze the convergence of the LOS angle error, we seek to find the closed-form solution of (14) by using the Frobenius method. Let $\beta \triangleq k_1 + 1 - k_2 > 0$, $\Theta = \{x|x = 2k + 1, k \in \mathbb{Z}\}$ as the set of all odd numbers, $\Omega = \{x|x = 2k, k \in \mathbb{Z}\}$ as the set of all even numbers; then, after some algebraic manipulations (please refer to Appendix A for the detailed derivation), the general closed-form solution of (14) can be readily obtained as

(a) If β is not an integer, then

$$e(t_{go}) = C_1 \sum_{i=0}^{\infty} a_i t_{go}^{i+k_1+1} + C_2 \sum_{i=0}^{\infty} b_i t_{go}^{i+k_2} \tag{18}$$

where the coefficients a_i and b_i are determined by

$$a_i = \begin{cases} \frac{(-k_3)^{i/2}}{f^{(0,i)}f^{(\beta,i)}}, & i \in \Omega \& i \geq 0 \\ 0, & i \in \Theta \& i > 0 \end{cases} \tag{19}$$

$$b_i = \begin{cases} \frac{(-k_3)^{i/2}}{f^{(0,i)}f^{(-\beta,i)}}, & i \in \Omega \& i \geq 0 \\ 0, & i \in \Theta \& i > 0 \end{cases}$$

(b) If β is an integer, then

$$e(t_{go}) = \begin{cases} C_1 \sum_{i=0}^{\infty} a_i t_{go}^{i+k_1+1} + C_2 \left[\ln t_{go} \sum_{i=0}^{\infty} a_i t_{go}^{i+k_1+1} \right. \\ \left. + \beta \sum_{i=-\beta, i \in \Omega}^{-2} \frac{g(\beta, -2-i)g(0, -2-i)}{(-k_3)^{-i/2}} t_{go}^{i+k_1+1} \right. \\ \left. - \sum_{i=0, i \in \Omega}^{\infty} (a_{i+2} \sum_{m=1}^{i/2+1} \frac{2(m+2)+\beta}{(m+2)(m+\beta+2)}) t_{go}^{i+k_1+3} \right], & \beta \in \Omega \\ C_1 \sum_{i=0}^{\infty} a_i t_{go}^{i+k_1+1} + C_2 \sum_{i=0}^{\infty} b_i t_{go}^{i+k_2}, & \beta \in \Theta \end{cases} \quad (20)$$

where the functions $f(x, y)$ and $g(x, y)$ are defined in (A10) and (A21), respectively, and C_1, C_2 are two integration constants determined by the initial conditions.

Observing (18) and (20), it is seen that the closed-form solutions have two different classes of LOS angle error trajectories depending on the difference in the root of the solution: one is the time-to-go polynomial error dynamics, and the other one is the error dynamics, which combine time-to-go polynomial with logarithmic functions. From these results, we have the following proposition to quantify the convergence of the LOS angle error and its rate.

Proposition 1. *The LOS angle error converges to zero at the time impact along the error dynamics in Equation (14) if $k_1 > 0$, and the LOS angle rate error converges to zero at the time impact along the error dynamics in (14) if $k_2 > 1$.*

Proof. Please refer to Appendix B for details. □

Since e converges to zero when $k_2 > 0$, the effect of the induced term $k_3 e$ gradually vanishes, and thus the error dynamics in (14) converge to the original one when the interceptor approaches the targets. Proposition 1 also implies that it would be wise to obey the condition $k_2 > 1$ in the homing phase so as to make the terminal LOS angle rate converge to zero, thus leading to a miss distance reduction.

4. Guidance Law Design

For surface/air-to-surface missile against non-maneuvering targets, it follows from (6); then, (14) reduces to

$$\ddot{\lambda} + \frac{a}{t_{go}} \dot{\lambda} + \left(\frac{b}{t_{go}^2} + k_3 \right) e = 0 \quad (21)$$

To force the system trajectory onto (21), we propose the following global sliding surface, which includes the LOS angle error and the LOS angle rate as

$$s = \dot{\lambda} + z \quad (22)$$

where

$$z = \int \left[\frac{a}{t_{go}} \dot{\lambda} + \left(\frac{b}{t_{go}^2} + k_3 \right) e \right] dt, z(0) = -\dot{\lambda} \quad (23)$$

where $a = k_1 + k_2$ and $b = (k_1 + 1)k_2$ are design parameters.

Differentiating (22) with respect to time yields

$$\dot{s} = -\frac{2\dot{r}\dot{\lambda}}{r} - \frac{a_M \cos \sigma}{r} + \frac{a}{t_{go}} \dot{\lambda} + \left(\frac{b}{t_{go}^2} + k_3 \right) e \quad (24)$$

The terminal angle control guidance law considering the target observability consists of an equivalent control term and an additional control term, which can be expressed as

$$a_M = a_M^{eq} + a_M^{add} \quad (25)$$

$$a_M^{eq} = \frac{1}{\cos \sigma} \left[-2\dot{r}\dot{\lambda} + \frac{a}{t_{go}} \dot{\lambda} r + \left(\frac{b}{t_{go}^2} + k_3 \right) er \right] \quad (26)$$

$$a_M^{add} = \frac{rKs \operatorname{sgn}(s)|a|^\alpha}{\cos \sigma} \quad (27)$$

where $K > 0$, $0 < \alpha < 1$ are design parameters of the guidance law. The term a_M^{eq} is known as the equivalent control part, which is derived by imposing $\dot{s} = 0$, while the add-on term a_M^{add} is designed for discontinuous switching, which is used to guarantee the convergence of the sliding dynamics and the robustness against unexpected disturbances.

Considering the system (21) and the sliding surface (22), the guidance law (25) is ensured, under the condition of enhanced target observability, for a limited time. To analyze the convergence of the LOS tracking angle error and the LOS angle rate of the missile in finite time under the guidance law (25), consider $V = 0.5s^2$ as a Lyapunov function candidate. Taking the time derivative of the Lyapunov function and substituting (24) into it yields

$$\begin{aligned} \dot{V} &= s \left(-\frac{2\dot{r}\dot{\lambda}}{r} - \frac{a_M \cos \sigma}{r} + \frac{a}{t_{go}} \dot{\lambda} + \left(\frac{b}{t_{go}^2} + k_3 \right) e \right) \\ &= -K|s|^{\alpha+1} \\ &\leq 0 \end{aligned} \quad (28)$$

which satisfies the Lyapunov stability criteria.

Due to the fact that $s(0) = 0$, one can conclude that the global sliding manifold is achieved, i.e., $s = 0$ holds during the entire homing engagement. This means that the observability improvement during the initial flight stage is ensured and the LOS motion can be easily predicted by using the obtained closed-form solution. This property is different from previous observability improvement guidance laws [28,29], where only ad hoc maneuvers perpendicular to the LOS are generated and the convergence pattern is not easy to predict. Additionally, since there is no requirement of extra energy in the reaching phase, one can safely predict that the proposed guidance law requires less of a control effort than other sliding mode control guidance laws.

Proposition 2. *The guidance command of the proposed guidance law converges to zero at the time of impact, i.e., $\lim_{t \rightarrow t_f} a_M = 0$, if $k_2 = 0$.*

Proof. Please refer to Appendix C for details. \square

Proposition 2 indicates that the limiting value of k_2 with the bounded acceleration command is 2. The lower gain will result in unbounded acceleration profiles, which will inevitably lead to a nonzero miss distance. A higher gain prevents the divergence of the guidance command near the interception of the target and, consequently, it reduces the terminal miss distance. Note that a stabilized acceleration for surface/air-to-surface tactical missiles is a crucial property to provide operational margins to cope with unexpected disturbances, especially near the interception.

5. Numerical Simulation

In this section, the performance of the proposed guidance law is investigated through numerical simulations under various conditions. To facilitate analysis, a point-mass missile model with a lag-free autopilot dynamics is used.

To verify the performance of the terminal angle control guidance law considering the target observability under different conditions, the parameters of the sliding surface and the guidance law changes. Table 1 provides the other related initial homing conditions that are used for simulations.

Table 1. Initial conditions for homing engagement.

Parameters	Values
Initial coordinates of the missile	(143.3 m, 4596.3 m)
Coordinates of the target	(4000 m, 0 m)
Missile velocity	300 m/s
Missile initial velocity angle	-30°
Maximum available overload	10 g

First, the feasibility of different target terminal impact angle constraints is studied. The parameters of the sliding surface and the guidance law take $k_1 = 3$, $k_2 = 2.5$, $\alpha = 0.8$, $K = 5$. The expected terminal impact angles are -40° , -50° and -60° , respectively. The simulation results are shown in Figure 2. In Figure 2, it can be seen that the terminal angle control guidance law, considering the target observability, can achieve different expected terminal attack angles. In order to enhance the observability of the target, the initial stage of the guidance needs a large acceleration command to bend the trajectory, which causes the LOS angle rate to oscillate. The LOS angle rate and acceleration command at the end of the guidance converge to zero, which is beneficial to the improvement of the guidance performance and robustness of the guidance law.

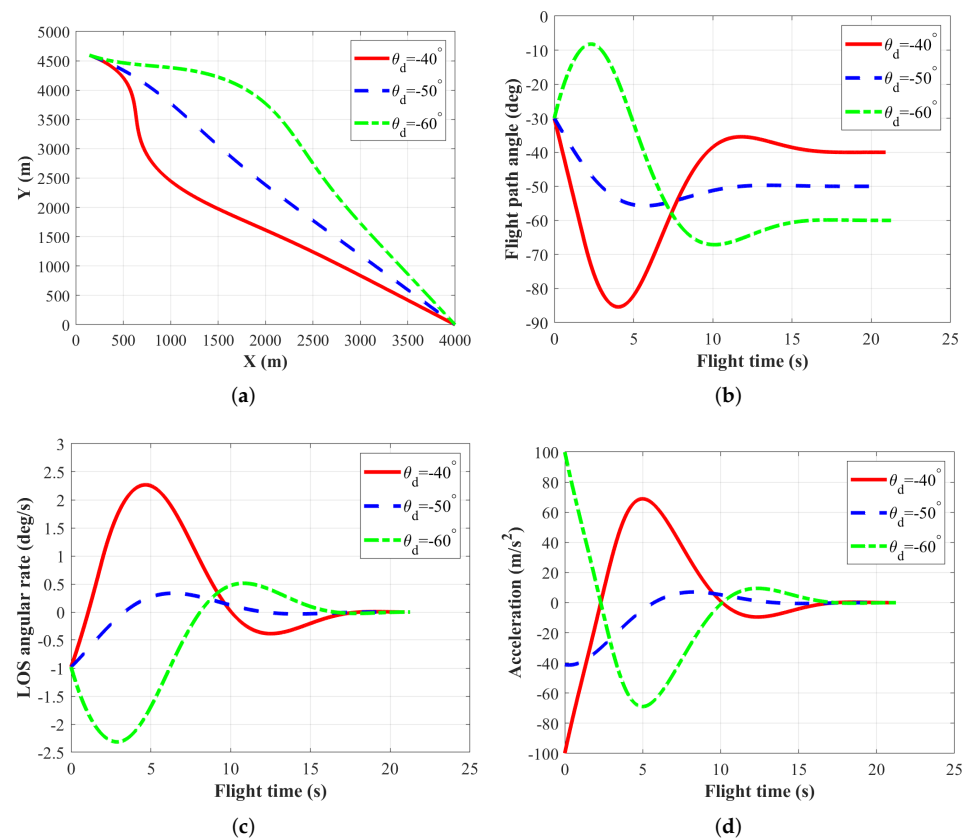


Figure 2. Simulation results under different expected terminal impact angles: (a) trajectory profiles; (b) flight path angle; (c) LOS angular rate; (d) acceleration command.

In order to further verify the validity of the proposed guidance law, the simulation compares the performance among the terminal angle control guidance law considering the target observability, trajectory shaping guidance (TSG) law [4] and the power function weighting optimal guidance (PFWOG) law [30]. The PFWOG law is obtained as the solution of a linear quadratic optimal control problem, with the energy cost weighted by a power of the remaining flight time. It produces different trajectories and command profiles depending on the choice of n . The acceleration command of the TSG and PFWOG law are determined in an expression as follows:

$$a_M = \begin{cases} 4V_M\dot{\lambda} + \frac{2V_M(\lambda-\theta_d)}{t_{go}} \\ -\frac{(n+2)(n+3)y}{t_{go}^2} - \frac{2(n+2)v}{t_{go}} \end{cases} \quad (29)$$

where the parameter n in the PFWOG law takes 1, the other parameters of the three guidance laws are the same as Table 1 and the desired terminal impact angle is -60° .

The comparative simulation results of the three guidance laws are depicted in Figure 3. As can be seen from those figures, all guidance laws can achieve the desired terminal impact angle, and the terminal's acceleration commands are all zero. Compared with the TSG and PFWOG law, the proposed guidance law can generate a larger LOS angular rate in the initial stage. Figure 4 shows that the target observability under the proposed guidance law is higher than that of the TSG and PFWOG law, but the disadvantage is that it needs a higher acceleration in the initial stage and more control energy.

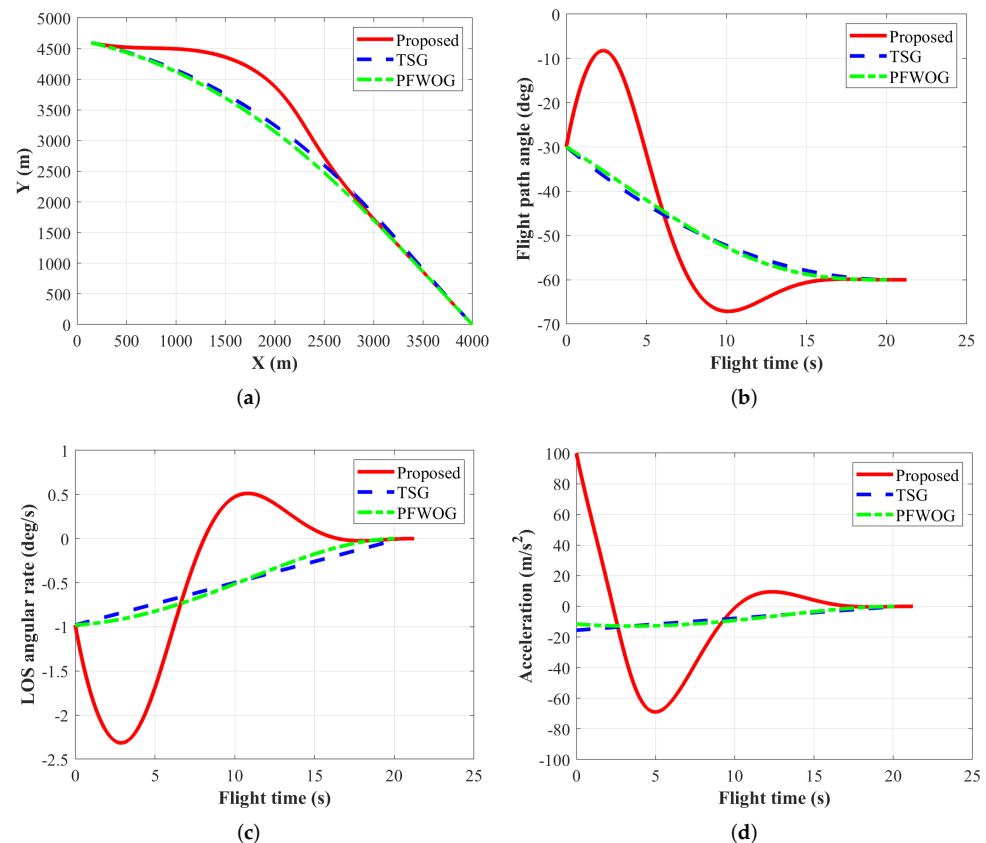


Figure 3. Comparative simulation results under different guidance laws: (a) trajectory profiles; (b) flight path angle; (c) LOS angular rate; (d) acceleration command.

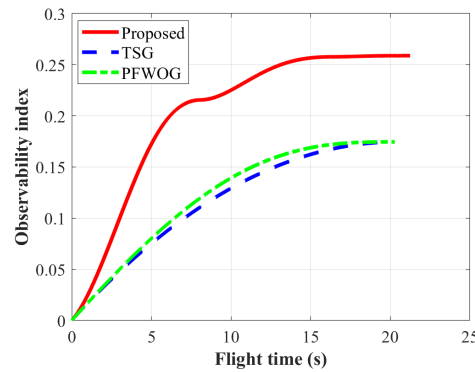


Figure 4. Observability index under different guidance laws.

At the same time, to validate the observability enhancement property of the proposed guidance law, UKF-embedded closed-loop simulations are performed to demonstrate the advantage of observability improvement. The state variables of this model are the relative position and the velocity in the inertial reference frame. Let $x_k = [x_k, y_k, v_{x,k}, v_{y,k}]^T$ and $a_{M_{x,k}} = [a_{M_{x,k}}, a_{M_{y,k}}]$. The missile acceleration (i.e., $a_{M_{x,k}}$ and $a_{M_{y,k}}$) is measured from a body-fixed accelerometer, which contains noise. The state transition of this model is determined as follows:

$$x_k = \Phi x_{k-1} + G a_{M,k-1} + G w_{k-1} \tag{30}$$

with

$$\Phi \triangleq \begin{bmatrix} I_{2 \times 2} & T_s I_{2 \times 2} \\ \mathbf{0}_{2 \times 2} & I_{2 \times 2} \end{bmatrix}, G \triangleq \begin{bmatrix} T_s^2 / 2 I_{2 \times 2} \\ I_{2 \times 2} \end{bmatrix} \tag{31}$$

where $T_s = 0.1$ s represents the sampling time and w_k denotes the system noise, which is considered as Gaussian white noise with a zero mean and variance as $Q_k = \text{diag}(\sigma_a^2, \sigma_a^2)$ and $\sigma_a = 1$ m/s². To initialize EKF, the state estimates and covariance for the guidance filter are used: $\hat{x}(0) = [143.3 \text{ m}, 4596.3 \text{ m}, 259.8 \text{ m/s}, 150.0 \text{ m/s}]^T$, $P(0) = \text{diag}([1000^2, 1000^2, 200^2, 200^2])$. In this paper, it is assumed that the measured LOS angle is accompanied by a Gaussian white noise with a zero mean and variance as $\sigma_m = 0.4^\circ$.

The estimation performance under the proposed guidance law, TSG and PFWOG law of 100 Monte-Carlo simulations are shown in Table 2. It can be clearly seen that the proposed guidance law can achieve a lower miss distance than the TSG and PFWOG law, which benefits from the improvement of target observability.

Table 2. Comparison of miss distance statistics under different laws.

Guidance Law	Average	Variance
TSG	174.256 m	189.215 m ²
PFWOG	163.194 m	178.531 m ²
Proposed	1.544 m	12.467 m ²

Finally, the performance of the terminal angle control guidance law considering the target observability under different k_2 and k_3 values is studied. The desired terminal impact angle is -60° . The simulation results are shown in Figure 5. The simulation results show that different k_2 and k_3 values cause different effects of ballistic oscillation. The design parameters of $k_1 = 1.5$, $k_3 = 0.1$ remain unchanged, and k_2 changes from 1, 2, 3 in Figure 5a,b. It can be found that, by comparing the simulation results, when $k_2 < 2$, the acceleration command of the guidance law cannot converge to zero at the guidance terminal. In Figure 5c,d, the design parameters of $k_1 = 1.5$, $k_2 = 3.0$ remain unchanged and k_3 changes from 0.05, 0.10, 0.15, where the k_3 value becomes increasingly larger. It is

obvious that the larger the LOS angular rate, the higher the missile acceleration, the more energy that is required and the higher the observability by comparing the simulation result.

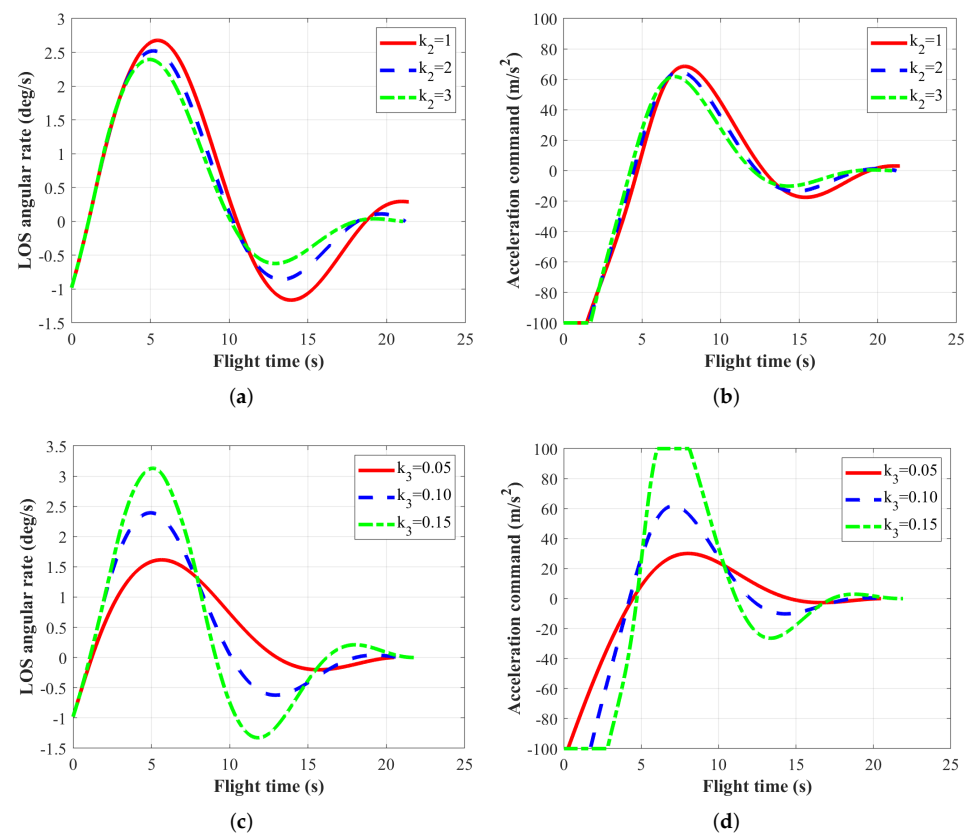


Figure 5. Comparative simulation results under different parameters: (a) LOS angular rate with different k_2 ; (b) acceleration command with different k_2 ; (c) LOS angular rate with different k_3 ; (d) acceleration command with different k_3 .

6. Conclusions

In this paper, the terminal impact angle control guidance problem of the stationary target, considering the target observability, is studied. Based on the sliding mode nonlinear control theory, which is robust to system uncertainty and external disturbance, the target observability is given under different constraints. Based on the criterion, new LOS angle error dynamics are proposed and their closed-loop analytical solution is solved. The terminal angle control guidance law with the global sliding model is designed by making the LOS oscillate in order to enhance the target observability. By analyzing the closed-loop analytical solution of the LOS angle error dynamics to obtain the design parameter $k_2 > 2$, the acceleration command of the guidance law can converge to zero at the guidance terminal. The method outlined is also suitable for a three-dimensional scenario, which can be analyzed in more detail in future research.

Author Contributions: Conceptualization, B.L. and P.T.; methodology, B.L.; software, B.L.; validation, B.L., H.X. and D.Z.; investigation, D.Z.; writing—original draft preparation, B.L.; writing—review and editing, P.T.; funding acquisition, D.Z. All authors have read and agreed to the published version of the manuscript.

Funding: This research was funded by Scientific and Technological Innovation 2030 under Grant 2021ZD0110900, National Natural Science Foundation of China (NSFC) under Grant 61903350.

Institutional Review Board Statement: Not applicable.

Informed Consent Statement: Not applicable.

Data Availability Statement: Not applicable.

Conflicts of Interest: The authors declare no conflict of interest.

Appendix A

The closed-form of the differential Equation (14), which can be analytically solved by the Frobenius method, and the obtained solutions, are in the form of a power series. To begin with, let the prime ' denote the derivative with respect to t_{go} . Then, Equation (14) can be reformulated as

$$t_{go}^2 e'' + t_{go}(k_1 + k_2)e' + [(k_1 + 1)k_2 + k_3 t_{go}^2]e = 0 \quad (A1)$$

Based on the concept of the Frobenius method, we seek a power series solution of the form

$$e(t_{go}) = \sum_{i=0}^{\infty} a_i t_{go}^{i+r}, a_0 \neq 0 \quad (A2)$$

where r may be any arbitrary number. Taking the first and second-order derivative of (A2) with respect to t_{go} and substituting them into (A1) gives

$$\sum_{i=0}^{\infty} [(i+r)(i+r-1) - (k_1 + k_2)(i+r) + (k_1 + 1)k_2] a_i t_{go}^{i+r} + k_3 \sum_{i=0}^{\infty} a_i t_{go}^{i+r+2} = 0 \quad (A3)$$

The indicial polynomial, which is the coefficient of the lowest power term t_{go}^r , is

$$[r(r-1) - r(k_1 + k_2) + (k_1 + 1)k_2] a_0 = 0 \quad (A4)$$

It is easy to obtain the solution of (A4) as

$$r_1 = k_1 + 1, r_2 = k_2 \quad (A5)$$

Since $r_1 > r_2$, we seek the first solution using r_1 . Substituting $r = k_1 + 1$ into (A3) and collecting the same power series results in

$$\sum_{i=0}^{\infty} i(i + \beta) a_i t_{go}^{i+k_1+1} + k_3 \sum_{i=0}^{\infty} a_i t_{go}^{i+k_1+3} = 0 \quad (A6)$$

Shifting the starting index from -2 gives

$$\sum_{i=-2}^{-1} (i+2)(i+\beta+2) a_{i+2} t_{go}^{i+k_1+3} + \sum_{i=0}^{\infty} [(i+2)(i+\beta+2) a_{i+2} + k_3 a_i] t_{go}^{i+k_1+3} = 0 \quad (A7)$$

For $i = -1$, the recurrence relation equation is $(\beta + 1) a_1 = 0$, which gives a natural selection of $a_1 = 0$. Without a loss of generality, we choose $a_0 = 1$.

For $i \geq 0$, the recurrence relation equation is

$$(i+2)(i+\beta+2) a_{i+2} + k_3 a_i = 0 \quad (A8)$$

which leads to the following two natural cases:

Case (1): $i \in \mathbb{N} \& i > 0$. Under this condition, it follows from (A8) and $a_1 = 0$ that $a_i = 0$.

Case (2): $i \in \mathbb{N} \& i \geq 0$. Under this condition, Equation (A8) gives a few coefficients as

$$\begin{aligned}
 a_2 &= \frac{-k_3}{2 \cdot (\beta + 2)}, a_4 = \frac{-k_3^2}{2 \cdot 4(\beta + 2) \cdot (\beta + 4)}, \\
 a_6 &= \frac{-k_3^3}{2 \cdot 4 \cdot 6(\beta + 2) \cdot (\beta + 4) \cdot (\beta + 6)}, \dots
 \end{aligned}
 \tag{A9}$$

Define $f(x, n)$ with $n = 0$, and

$$f(x, n) = (x + 2) \cdot (x + 4) \cdot \dots \cdot (x + n)
 \tag{A10}$$

with n being positive even numbers.

Then, the coefficients for Case (2) can be rewritten as

$$a_i = \frac{(-k_3)^{i/2}}{f(0, i) \cdot f(\beta, i)}
 \tag{A11}$$

Therefore, the first solution can be obtained by combining Cases (1) and (2) as

$$\begin{aligned}
 e(t_{go}) &= \sum_{i=0}^{\infty} a_i t_{go}^{i+k_1+1} \\
 a_i &= \begin{cases} \frac{(-k_3)^{i/2}}{f(0, i) f(\beta, i)}, & i \in \Omega \& i \geq 0 \\ 0, & i \in \Theta \& i > 0 \end{cases}
 \end{aligned}
 \tag{A12}$$

To derive the second solution using the Frobenius method, the following two conditions depending on the nature of the roots of (A4) are considered.

Condition (1): Distinct roots not differing by an integer, i.e., β is not an integer. Under this condition, the second solution can be obtained by substituting $r = k_2$ into (A3). Following the same lines as shown above, one can imply that

$$\begin{aligned}
 e(t_{go}) &= \sum_{i=0}^{\infty} b_i t_{go}^{i+k_2} \\
 b_i &= \begin{cases} \frac{(-k_3)^{i/2}}{f(0, i) f(-\beta, i)}, & i \in \Omega \& i \geq 0 \\ 0, & i \in \Theta \& i > 0 \end{cases}
 \end{aligned}
 \tag{A13}$$

Condition (2): Roots differing by an integer, i.e., β is an integer. Under this condition, the second solution has the following form:

$$e_2(t_{go}) = C e_1(t_{go}) \ln t_{go} + \sum_{i=0}^{\infty} b_i t_{go}^{i+k_2}
 \tag{A14}$$

where $C > 0$ is a constant.

Taking the first and second-order derivative of (A14) and substituting them into (A1) gives

$$\begin{aligned}
 &C \ln t_{go} \left\{ t_{go}^2 e_1''(t_{go}) + t_{go} (k_1 + k_2) e_1'(t_{go}) + \right. \\
 &\left. [(k_1 + 1)k_2 + k_3 t_{go}^2] e_1(t_{go}) \right\} + C [2t_{go} e_1'(t_{go}) - \\
 &(k_1 + k_2 + 1) e_1(t_{go})] + \sum_{i=0}^{\infty} i(i - \beta) b_i t_{go}^{i+k_2} + k_3 \sum_{i=0}^{\infty} b_i t_{go}^{i+k_2+2} = 0
 \end{aligned}
 \tag{A15}$$

Since $e_1(t_{go})$ is a basic solution of (A1), the term multiplied by the logarithmic function equals zero. Shifting the starting index from $-\beta - 2$ for (A15) gives

$$\begin{aligned}
 & C[2t_{go}e_1'(t_{go}) - (k_1 + k_2 + 1)e_1(t_{go})] + \\
 & \sum_{i=-\beta-2}^{-\beta-1} (i + \beta + 2)(i + 2)b_{i+\beta+2}t_{go}^{i+k_1+3} + \\
 & \sum_{i=-\beta}^{\infty} [(i + \beta + 2)(i + 2)b_{i+\beta+2} + k_3b_{i+\beta}]t_{go}^{i+k_1+3} = 0
 \end{aligned} \tag{A16}$$

It is easy to verify that the lowest power series of the term $[2t_{go}^2e_1'(t_{go}) - (k_1 + k_2 + 1)e_1(t_{go})]$ is $t_{go}^{k_1+1}$. Moreover, the term $[2t_{go}^2e_1'(t_{go}) - (k_1 + k_2 + 1)e_1(t_{go})]/t_{go}^{k_1+1}$ only has even power series. Rewriting (A16) in power series as

$$\begin{aligned}
 & \sum_{i=-2}^{\infty} [Ca_{i+2}(2i + \beta + 4)]t_{go}^{i+k_1+3} + \\
 & \sum_{i=-\beta-2}^{-\beta-1} (i + \beta + 2)(i + 2)b_{i+\beta+2}t_{go}^{i+k_1+3} + \\
 & \sum_{i=-\beta}^{\infty} [(i + \beta + 2)(i + 2)b_{i+\beta+2} + k_3b_{i+\beta}]t_{go}^{i+k_1+3} = 0
 \end{aligned} \tag{A17}$$

Next, we consider the following two cases.

Case (1): β is a positive even number. For this case, it follows from (A17) that $b_0 \neq 0$, $b_1 = 0$, and, therefore, the coefficients satisfy

$$b_j \begin{cases} \neq 0, & j \in \Omega \& j \geq 0 \\ = 0, & j \in \Theta \& j > 0 \end{cases} \tag{A18}$$

From (A17), the coefficient $b_{\beta-2}$ can be obtained by equating the coefficient of the power series $t_{go}^{k_1+1}$ from (A17) to zero as

$$C\beta + k_3b_{\beta-2} = 0 \Rightarrow b_{\beta-2} = -\frac{C\beta}{k_3} \tag{A19}$$

Then, for $i \leq -2$, the coefficients can be calculated backward from $b_{\beta-2}$, whereas the coefficients with $i \geq 0$ can be obtained forward from b_{β} .

For $i \leq -2$, the recurrence relation equation is

$$(i + \beta + 2)(i + 2)b_{i+\beta+2} + k_3b_{i+\beta} = 0 \tag{A20}$$

Define $g(x, n)$ with $n = 0$, and

$$g(x, n) = g(x - 2) \cdot g(x - 4) \cdot \dots \cdot g(x - n) \tag{A21}$$

with n being positive even numbers.

Then, combining (A18) and (A20) gives

$$b_{i+\beta} = \frac{C\beta g(\beta, -2 - i)g(0, -2 - i)}{(-k_3)^{-i/2}} \tag{A22}$$

For $i \geq 0$, the recurrence relation equation is

$$Ca_{i+2}(2i + \beta + 4) + (i + \beta + 2)(i + 2)b_{i+\beta+2} + k_3b_{i+\beta} = 0 \tag{A23}$$

which gives the following coefficients

$$b_{i+\beta+2} = a_{i+2}b_\beta - Ca_{i+2} \sum_{m=1}^{i/2+1} \frac{2(m+2) + \beta}{(m+2)(m+\beta+2)} \tag{A24}$$

Substituting (A22) and (A24) into (A14) yields

$$\begin{aligned} e_2(t_{go}) &= Ce_1(t_{go}) \ln t_{go} + \sum_{i=-\beta}^{-2} b_{i+\beta} t_{go}^{i+k_1+1} + b_\beta t_{go}^{k_1+1} \\ &+ \sum_{i=2}^{\infty} b_{i+\beta} t_{go}^{i+k_1+1} \\ &= Ce_1(t_{go}) \ln t_{go} + \sum_{i=-\beta}^{-2} b_{i+\beta} t_{go}^{i+k_1+1} + b_\beta a_0 t_{go}^{k_1+1} \\ &+ \sum_{i=0}^{\infty} b_{i+\beta+2} t_{go}^{i+k_1+3} \\ &= b_\beta \sum_{i=0}^{\infty} a_i t_{go}^{i+k_1+1} + C [e_1(t_{go}) \ln t_{go} \\ &+ \beta \sum_{i=-\beta, i \in \Omega}^{-2} \frac{g(\beta, -2-i)g(0, -2-i)}{(-k_3)^{-i/2}} t_{go}^{i+k_1+1} \\ &- \sum_{i=0, i \in \Omega}^{\infty} \left(a_{i+2} \sum_{m=1}^{i/2+1} \frac{2(m+2) + \beta}{(m+2)(m+\beta+2)} \right) t_{go}^{i+k_1+3}] \end{aligned} \tag{A25}$$

Since C and b_β are two arbitrary constants, Equation (A25) is an incomplete equation. However, observing that the term multiplied by b_β is the first basis solution, then, the second linearly independent solution of (A1) is

$$\begin{aligned} e_2(t_{go}) &= e_1(t_{go}) \ln t_{go} + \\ &\beta \sum_{i=-\beta, i \in \Omega}^{-2} \frac{g(\beta, -2-i)g(0, -2-i)}{(-k_3)^{-i/2}} t_{go}^{i+k_1+1} - \\ &\sum_{i=0, i \in \Omega}^{\infty} \left(a_{i+2} \sum_{m=1}^{i/2+1} \frac{2(m+2) + \beta}{(m+2)(m+\beta+2)} \right) t_{go}^{i+k_1+3} \end{aligned} \tag{A26}$$

Case (2): β is a positive odd number. In this case, consider the following two subcases.

Subcase (1): $\beta = 1$. Under this condition, equating the coefficient of the power series $t_{go}^{k_1+1}$ from (A17) to zero gives

$$C\beta + (1 - \beta)b_1 = 0 \Rightarrow C = 0 \tag{A27}$$

Then, the basic solution $e_2(t_{go})$ reduces to

$$e_2(t_{go}) = \sum_{i=0}^{\infty} b_i t_{go}^{i+k_2} \tag{A28}$$

which is the same as Condition (1) and thus shares the same solution.

Subcase (2): $\beta > 1$. Under this condition, equating the coefficient of the power series $t_{go}^{k_1+1}$ from (A17) to zero gives

$$C\beta + k_3 b_{\beta-2} = 0 \Rightarrow b_{\beta-2} = -\frac{C\beta}{k_3} \tag{A29}$$

Since $\beta > 1$, it follows from (A17) that $b_0 \neq 0, b_1 = 0$ and the recurrence relation equation for $i \leq \beta - 2$ is

$$(i + \beta + 2)(i + 2)b_{i+\beta+2} + k_3b_{i+\beta} = 0 \tag{A30}$$

which means that

$$b_{\beta-2} = b_{\beta-4} = \dots = b_3 = b_1 = 0 \tag{A31}$$

Combining (A29) and (A31) leads to $C = 0$. Then, the basic solution $e_2(t_{go})$ reduces to

$$e_2(t_{go}) = \sum_{i=0}^{\infty} b_i t_{go}^{i+k_2} \tag{A32}$$

which is the same as Condition (1) and thus shares the same solution.

Finally, by summarizing the above results, the closed-form solution of (A1) is

(a) If β is not an integer, then

$$e(t_{go}) = C_1 \sum_{i=0}^{\infty} a_i t_{go}^{i+k_1+1} + C_2 \sum_{i=0}^{\infty} b_i t_{go}^{i+k_2} \tag{A33}$$

where

$$a_i = \begin{cases} \frac{(-k_3)^{i/2}}{f(0,i)f(\beta,i)}, & i \in \Omega \& i \geq 0 \\ 0, & i \in \Theta \& i > 0 \end{cases} \tag{A34}$$

$$b_i = \begin{cases} \frac{(-k_3)^{i/2}}{f(0,i)f(-\beta,i)}, & i \in \Omega \& i \geq 0 \\ 0, & i \in \Theta \& i > 0 \end{cases}$$

(b) If β is an integer, then

$$e(t_{go}) = \begin{cases} C_1 \sum_{i=0}^{\infty} a_i t_{go}^{i+k_1+1} + C_2 \left[\ln t_{go} \sum_{i=0}^{\infty} a_i t_{go}^{i+k_1+1} \right. \\ \left. + \beta \sum_{i=-\beta, i \in \Omega}^{-2} \frac{g(\beta, -2-i)g(0, -2-i)}{(-k_3)^{-i/2}} t_{go}^{i+k_1+1} \right. \\ \left. - \sum_{i=0, i \in \Omega}^{\infty} (a_{i+2} \sum_{m=1}^{i/2+1} \frac{2(m+2)+\beta}{(m+2)(m+\beta+2)}) t_{go}^{i+k_1+3} \right], & \beta \in \Omega \\ C_1 \sum_{i=0}^{\infty} a_i t_{go}^{i+k_1+1} + C_2 \sum_{i=0}^{\infty} b_i t_{go}^{i+k_2}, & \beta \in \Theta \end{cases} \tag{A35}$$

where C_1, C_2 are two integration constants determined by the initial conditions.

Appendix B

It is easy to verify that the lowest power terms of (18) are $t_{go}^{k_1+1}, t_{go}^{k_2}$, whereas the lowest power terms of (20) are $t_{go}^{k_1+1}, t_{go}^{k_1+1} \ln t_{go}, t_{go}^{k_2}$.

For any $\varepsilon > 0$, using L'Hospital's rule, one can imply that

$$\lim_{x \rightarrow 0^+} x^\varepsilon \ln x = \lim_{x \rightarrow 0^+} \frac{\ln x}{x^{-\varepsilon}} = \lim_{x \rightarrow 0^+} \frac{x^{-1}}{-\varepsilon x^{-1-\varepsilon}} \tag{A36}$$

$$= \lim_{x \rightarrow 0^+} \left(-\frac{1}{\varepsilon} x^\varepsilon \right) = 0$$

Then, the lowest order in t_{go} of $e(t_{go})$ is larger than zero if $k_1 > -1, k_2 > 0$, whereas the lowest order in t_{go} of $\dot{e}(t_{go})$ is larger than zero if $k_1 > 0, k_2 > 1$. Next, in cooperation with the condition $k_1 + 1 > k_2$, the proof is completed.

Appendix C

It follows from (26) that the lowest power term of t_{go} in (26) is one order power less than t_{go} of $\dot{e}(t_{go})$ or two power order than $e(t_{go})$. Moreover, Proposition 1 reveals that it converges to zero if $k_1 > 0, k_2 > 1$. Combining the property of the global sliding manifold, i.e., $s = 0$, with $k_1 + 1 > k_2$ leads to the proof.

References

1. Siouris, G.M. *Missile Guidance and Control Systems*; Springer: New York, NY, USA, 2004; pp. 194–205.
2. Li, B.; Lin, D.; Wang, J. Guidance law to control impact angle and time based on optimality of error dynamics. *Proc. Inst. Mech. Eng. Part G J. Aerosp. Eng.* **2019**, *233*, 3577–3588. [[CrossRef](#)]
3. Hou, Z.; Yang, Y.; Liu, L. Terminal sliding mode control based impact time and angle constrained guidance. *Aerosp. Sci. Technol.* **2019**, *93*, 105142. [[CrossRef](#)]
4. Zarchan, P. *Tactical and Strategic Missile Guidance*; American Institute of Aeronautics and Astronautics, Inc.: Reston, VA, USA, 2012; pp. 569–576.
5. Kim, B.S.; Lee, J.G.; Han, H.S. Biased PNG law for impact with angular constraint. *IEEE Trans. Aerosp. Electron. Syst.* **1998**, *34*, 277–288.
6. Erer, K.S.; Merttopcuoglu, O. Indirect Impact-Angle-Control Against Stationary Targets Using Biased Pure Proportional Navigation. *J. Guid. Control Dyn.* **2012**, *35*, 700–704. [[CrossRef](#)]
7. Kim, H.-G.; Lee, J.-Y. Generalized Guidance Formulation for Impact Angle Interception with Physical Constraints. *Aerospace* **2021**, *8*, 307. [[CrossRef](#)]
8. Zhao, S.; Chen, W.; Yang, L. Optimal Guidance Law with Impact-Angle Constraint and Acceleration Limit for Exo-Atmospheric Interception. *Aerospace* **2021**, *8*, 358. [[CrossRef](#)]
9. Utkin, V.I. *Sliding Modes in Control and Optimization*; Springer: Berlin/Heidelberg, Germany, 1992; pp. 240–249.
10. Zhang, Z.; Li, S.; Sheng, L. Terminal guidance laws of missile based on ISMC and NDOB with impact angle constraint. *Aerosp. Sci. Technol.* **2013**, *31*, 30–41. [[CrossRef](#)]
11. Guo, J.; Xiong, Y.; Zhou, J. A New Sliding mode Control Design for Integrated Missile Guidance and Control System. *Aerosp. Sci. Technol.* **2018**, *78*, 54–61. [[CrossRef](#)]
12. He, S.; Song, T.; Lin, D. Impact Angle Constrained Integrated Guidance and Control for Maneuvering Target Interception. *J. Guid. Control Dyn.* **2017**, *40*, 2653–2661. [[CrossRef](#)]
13. Zhou, D.; Mu, C.; Xu, W. Adaptive Sliding-Mode Guidance of a Homing Missile. *J. Guid. Control Dyn.* **2015**, *22*, 589–594. [[CrossRef](#)]
14. Kumar, S.R.; Ghose, D. Sliding mode control based terminal impact angle constrained guidance laws using dual sliding surfaces. In Proceedings of the 2013 American Control Conference, Washington, DC, USA, 17–19 June 2013.
15. Lee, C.-H.; Tahk, M.-J.; Lee, J.-I. Design of impact angle control guidance laws via high-performance sliding mode control. *Proc. Inst. Mech. Eng. Part G J. Aerosp. Eng.* **2013**, *227*, 235–253. [[CrossRef](#)]
16. Lingren, A.G.; Gong, K.F. Position and Velocity Estimation Via Bearing Observations. *IEEE Trans. Aerosp. Electron. Syst.* **1978**, *14*, 564–577. [[CrossRef](#)]
17. Jiang, H.; Cai, Y.; Yu, Z. Observability Metrics for Single-Target Tracking With Bearings-Only Measurements. *IEEE Trans. Syst. Man. Cybern.* **2020**, *99*, 1–13. [[CrossRef](#)]
18. Xu, S.; Dogancay, K. Optimal Sensor Placement for 3-D Angle-of-Arrival Target Localization. *IEEE Trans. Aerosp. Electron. Syst.* **2017**, *53*, 1196–1211. [[CrossRef](#)]
19. Grzymisch, J.; Fichter, W. Observability Criteria and Unobservable Maneuvers for In-Orbit Bearings-Only Navigation. *J. Guid. Control Dyn.* **2014**, *37*, 1250–1259. [[CrossRef](#)]
20. Taek, L.S.; Tae, Y.U. Practical guidance for homing missiles with bearings-only measurements. *IEEE Trans. Aerosp. Electron. Syst.* **1996**, *32*, 434–443. [[CrossRef](#)]
21. Lee, H.-I.; Shin, H.-S.; Tsourdos, A. Weaving Guidance for Missile Observability Enhancement. *Ifac Papersonline* **2017**, *50*, 15197–15202. [[CrossRef](#)]
22. Lee, C.-H.; Kim, T.-H.; Tahk, M.-J. Biased PNG for target observability enhancement against nonmaneuvering targets. *IEEE Trans. Aerosp. Electron. Syst.* **2015**, *51*, 2–17. [[CrossRef](#)]
23. Wang, Y.; Wang, J.; He, S. Optimal Guidance With Active Observability Enhancement for Scale Factor Error Estimation of Strapdown Seeker. *IEEE Trans. Aerosp. Electron. Syst.* **2021**, *57*, 4347–4362. [[CrossRef](#)]
24. Kim, T.-H.; Lee, C.-H.; Tahk, M.-J. Time-to-go Polynomial Guidance with Trajectory Modulation for Observability Enhancement. *IEEE Trans. Aerosp. Electron. Syst.* **2013**, *49*, 55–73. [[CrossRef](#)]
25. Hull, D.; Speyer, J.; Burris, D. Linear-quadratic guidance law for dual control of homing missiles. *J. Guid. Control Dyn.* **1990**, *13*, 137–144. [[CrossRef](#)]
26. He, S.; Shin, H.S.; Ra, W.S. Observability-Enhancement Optimal Guidance Law. In Proceedings of the 2019 Workshop on Research, Education and Development of Unmanned Aerial Systems, Cranfield, UK, 25–27 November 2019.

27. Nardone, S.C.; Aidala, V.J. Observability Criteria for Bearings-Only Target Motion Analysis. *IEEE Trans. Aerosp. Electron. Syst.* **1981**, *17*, 162–166. [[CrossRef](#)]
28. Lee, H.-I.; Tahk, M.-J.; Sun, B.-C. Practical Dual-Control Guidance Using Adaptive Intermittent Maneuver Strategy. *J. Guid. Control Dyn.* **2001**, *24*, 1009–1015. [[CrossRef](#)]
29. Seo, M.-G.; Tahk, M.-J. Observability analysis and enhancement of radome aberration estimation with line-of-sight angle-only measurement. *IEEE Trans. Aerosp. Electron. Syst.* **2015**, *51*, 3322–3331.
30. Ryoo, C.-K.; Cho, H.; Tahk, M.-J. Time-to-go weighted optimal guidance with impact angle constraints. *IEEE Trans. Control Syst. Technol.* **2006**, *14*, 483–492. [[CrossRef](#)]